CO Chemiluminescence and Kinetics of the $C_2 + O_2$ Reaction

Arthur Fontijn,* Abel Fernandez, Aleksandra Ristanovic, Mai Y. Randall, and Jerome T. Jankowiak

High-Temperature Reaction Kinetics Laboratory, The Isermann Department of Chemical Engineering, Rensselaer Polytechnic Institute, Troy, New York 12180-3590

Received: September 28, 2000; In Final Form: January 9, 2001

The reaction $C_2(X^1\Sigma, a^3\Pi) + O_2(X^3\Sigma) \rightarrow CO(X^1\Sigma, A^1\Pi, a'\,^3\Sigma, d^3\Delta, e^3\Sigma) + CO(X^1\Sigma)$ has been studied in two types of reactors. A Pyrex steady-state fast-flow reactor at approximately 500 K was used to obtain the spectral distributions of the CO ($A^1\Pi-X^1\Sigma$) emissions in the vacuum ultraviolet (VUV) and the CO triplet states emissions in the visible and near-IR (vis) wavelength region. The VUV emission had not previously been positively identified. The C_2 was produced from the $C_2Cl_4 + K$ reaction. In a pseudostatic high-temperature photochemistry (HTP) reactor C_2 was made by 193 nm multiphoton dissociation of C_2Cl_4. That apparatus was used for quenching and rate coefficient experiments in the time domain. The VUV quenching measurements confirm the orbital symmetry argument that the reaction proceeds through excited C_2O_2 intermediates. Reaction schemes for $C_2(X^1\Sigma)$ and for $C_2(a^3\Pi)$ are presented. The results are compared to those from the $O + C_2H_2$ reaction, which leads via $C_2O + O$ to the same band systems emissions, and the differences are discussed. Measurements of the overall rate coefficients from the decrease of the vis chemiluminescence intensities with time yielded $k_{vis}(298-711\ K) = 1.1 \times 10^{-11} \exp(-381\ K/T)\ cm^3\ molecule^{-1}\ s^{-1}$, with 2σ precision limits of around ±5% and corresponding estimated accuracy limits of about ±21%. This expression is in excellent agreement with earlier rate coefficient values determined by different methods. The VUV experiments yielded slightly higher values, the reason for which is uncertain. It is speculated that an apparent continuum observed in the VUV spectra could be $^1C_2O_2$ excimer radiation to the repulsive ground state.

Introduction

CO chemiluminescence has been encountered in many environments. It has most frequently been studied in hydrocarbon flames[1] and, near room temperature, in the $O + C_2H_2$ and C_3O_2 reactions, where the chemiexcitation has been shown to result from an $O + C_2O$ mechanism.[2−6] Emission has been observed from the fourth positive CO ($A^1\Pi-X^1\Sigma$), Herman ($e^3\Sigma-a^3\Pi$), triplet ($d^3\Delta-a^3\Pi$), and Asundi ($a'\,^3\Sigma-a^3\Pi$) bands,[3] as well as from the forbidden Cameron ($a^3\Pi-X^1\Sigma$) bands.[5] See Figure 1, from the data of Tilford and Simmons,[7] for identification of these states and the observed band systems. Assuming O and C_2O to be in their ground states, 8.95 eV is available from their reaction to excite one of the product CO molecules to one of these states.[6] Even more excitation energy is available from

$$C_2(X^1\Sigma, a^3\Pi) + O_2(X^3\Sigma) \rightarrow 2CO \qquad (1)$$

which is 10.84 and 10.92 eV exothermic, for $C_2(X^1\Sigma)$ and $C_2(a^3\Pi)$, respectively.[6] These states are hereafter referred to as $^1C_2$ and $^3C_2$. The chemiluminescence from this reaction has not often been studied. Filseth et al.[9] established the presence of vacuum ultraviolet (VUV) emission, which they assumed to be due to the CO ($A^1\Pi-X^1\Sigma$) fourth positive (4+) system, and also observed visible emissions. Reisler, Mangir, and Wittig (RMW)[10] identified the visible emissions as the Herman, Triplet, and Asundi bands and performed further studies (MRW).[11] Generally, both $^1C_2$ and $^3C_2$ are present and it has been proven difficult to assign the observations to one or the other of these states, which rapidly equilibrate in the presence of O_2.[10−12]

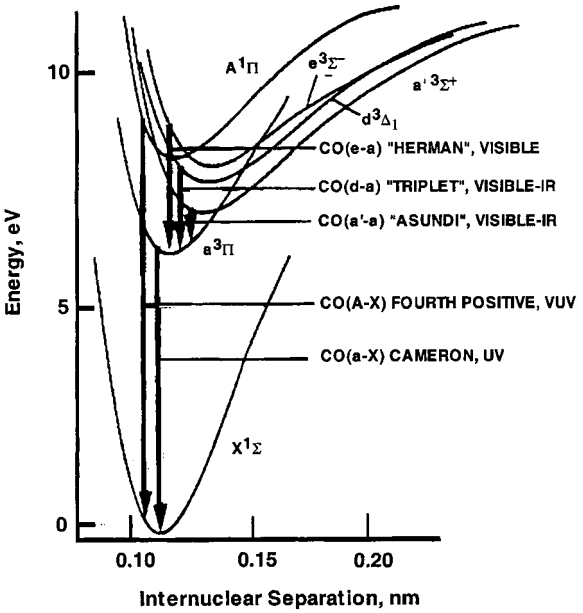

Figure 1. CO potential curves and transitions. Generated by W. L. Dimpfl, Spectral Sciences, Inc., from scaled traces of Figure 3 of Tilford and Simmons.[7]

A number of measurements of k_1 have been performed, both at room temperature[9,10,13,14] and in the 298−1300 K temperature range.[12,15] Laser-induced fluorescence (LIF) of $^1C_2$ and $^3C_2$ or chemiluminescence were used for these studies. A 2750−3950 K shock tube study has also been reported.[16]

The present work was undertaken to identify the VUV spectrum, which is shown to be that of the 4+ system, and to

10.1021/jp003529r CCC: $20.00
Published on Web 02/24/2001

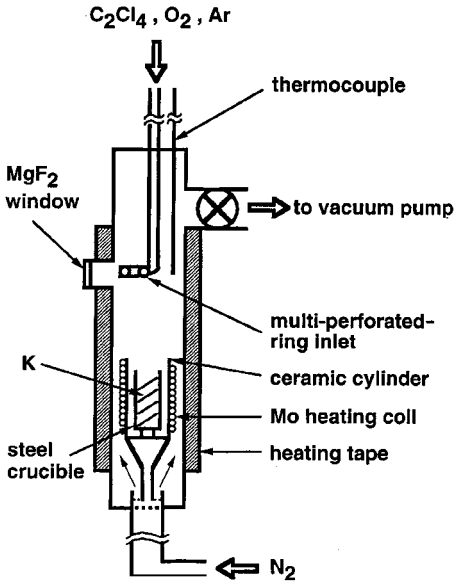

Figure 2. Schematic of the Pyrex fast-flow reactor.

obtain further insight into the mechanisms leading to it and to the triplet systems emissions. The mechanisms involved are compared to those leading to the same band systems[5] in the O + C_2O reaction. There $A^1\Pi$ state molecules are formed predominantly by collision-induced cross-relaxation from CO triplet states,[4,6] the formation of which is thought to proceed through a C_2O_2* intermediate.[6] RMW have concluded on the basis of orbital symmetry arguments that reaction 1 cannot be a concerted four-center reaction but has to involve a C_2O_2* complex.[10] Experimental evidence for this is presented here. In practical contexts, especially the emission of the CO 4+ system is of interest for a variety of combustion monitoring applications[1] and for high-altitude rocket plume research.

Technique

Three types of experiments have been performed. In the first of these, a steady-state fast-flow reactor was employed to measure spectral distributions and C_2 was produced by using potassium vapor to strip Cl from C_2Cl_4.[17] This setup, while convenient for obtaining spectra, did not lend itself well to establishing the pressure dependence of the intensities of the various band systems or to rate coefficient measurements. Such measurements were obtained in the time domain in an HTP (high-temperature photochemistry) reactor. This type of reactor is operated in a pseudostatic mode. It has been frequently used for obtaining temperature-dependent rate coefficients, $k(T)$, using atomic absorption and fluorescence, and LIF.[18−23] The associated diagnostic equipment was adapted here to make wavelength-integrated chemiluminescence measurements in the vacuum ultraviolet and simultaneously in the visible. For these observations C_2 was produced by 193 nm multiphoton dissociation (MPD) of C_2Cl_4 or in some cases C_2H_2. Finally, in a few experiments the CO 4+ spectrum from $C_2 + O_2$ was compared to that from O + C_2H_2. The latter was obtained in a microwave discharge flow reactor of the same design as used in our previous studies of the chemiluminescence from that reaction.[4,6] This reactor is not discussed further here.

Fast-Flow Reactor Experiments. A 3.5 cm i.d. Pyrex fast-flow reactor, equipped with a MgF_2 window, Figure 2, was used to obtain $C_2 + O_2$ chemiluminescence spectra. Nitrogen bath gas flows through the annular region between a movable 2.2 cm i.d. ceramic cylinder and the reactor wall. Further downstream, the nitrogen entrains potassium vapor. The potassium is contained at about 540 K in a 1.8 cm i.d. stainless steel crucible (2.1 cm o.d.), which rests inside the ceramic cylinder. Heating tape is wrapped around the reactor to prevent potassium vapor from condensing on the inner Pyrex wall. Temperature in the observation zone was kept at about 500 K, as measured with a retractable Pt/Pt−13% Rh thermocouple. C_2Cl_4 and O_2 are introduced through a multiperforated-ring inlet. Teledyne-Hastings HFC-202 mass flow controllers were used to control and measure the gas flows. The reactor pressure was measured by an MKS Baratron transducer.

Most spectral measurements were obtained using a Princeton Instruments 1024-EM VUV thermoelectrically cooled CCD camera mounted onto a Minuteman 305-M 0.5 m Czerny−Turner vacuum monochromator. Flat reflection gratings blazed for either 150 or 500 nm were used. The operating temperature used for the CCD array was −50 °C. To allow for VUV measurements and to prevent water from condensing on the CCD array, the monochromator is connected to a liquid nitrogen trap and is maintained at a pressure $<1.3 \times 10^{-6}$ bar by a diffusion pump, as measured by a Televac B2A pressure gauge. The CCD array is coated by the manufacturer with a proprietary substance, lumogen, which fluoresces from 500 to 700 nm to enable detection down to 110 nm. The maximum detectable wavelength is around 900 nm. The analogue output of the CCD camera is digitized and processed by a Princeton Instruments ST-138 controller, sent to a computer, using Princeton Instruments WinSpec/32 version 2.1 software, to store and display the spectral data.

The independence of the CCD signal intensity as a function of pixel position was verified by varying the monochromator position randomly and measuring the intensity of a single peak. The peaks were tested at 151.0, 172.9, 181.4, 404.7, and 435.9 nm. To obtain a good S/N, the spectral measurements were performed using a CCD exposure time of 30 s.

An unsatisfactory characteristic of the CCD camera is its loss of sensitivity with time. After about 0.5 h of operation, the sensitivity of the detector in the VUV is halved. To compensate for this loss of sensitivity the spectral measurements are made in random order with respect to monochromator wavelength position. This method also compensates for the decrease in chemiluminescence intensities from the decrease of the potassium concentration with time, due to the decrease of its level in the crucible. As time progressed, further deterioration made it impractical to continue working with the CCD camera in the VUV. Instead an EMI 9403B PMT was used, though it had a lower sensitivity.

The gases used were Ar (99.998%) and N_2 (99.995%), both from the liquid, supplied by Praxair. O_2 (UHP, 99.98%) and 5.08% O_2 ("Extra Dry" 99.6% in Ar (99.999%)) were obtained from Matheson, and the 99.6% C_2H_2 was from Liquid Carbonic. Potassium chunks 98% and liquid C_2Cl_4 were supplied by Aldrich. The C_2Cl_4 was purified and degassed by bulb-to-bulb distillation. C_2Cl_4/Ar mixtures were prepared in the laboratory.

HTP Experiments. A schematic of the reactor is shown in Figure 3. The basic layout and equipment are the same as used in earlier studies. The 5 cm i.d., 30 cm long ceramic reaction tube is surrounded by resistance heating elements and insulation in a stainless steel vacuum chamber. The bottom (upstream) plate contains an inlet for Ar bath gas and an air-cooled inlet for introduction of the reactant gases. Teledyne-Hastings mass flow controllers are employed, and pressure is measured with an MKS Baratron transducer. The slow gas velocities, 2−20

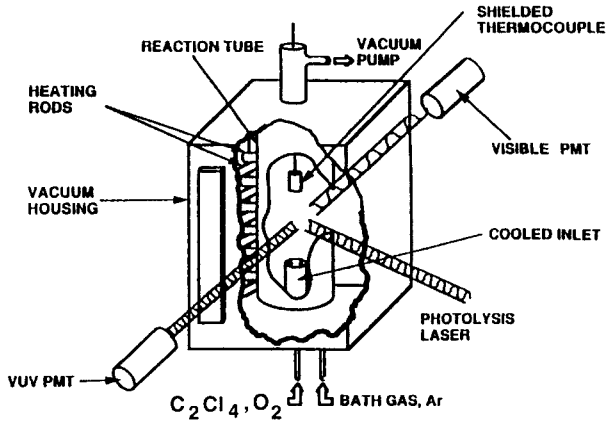

Figure 3. Schematic of the high-temperature photochemistry reactor.

cm s^{-1}, used are fast enough to provide each photolysis pulse with a fresh reactant mixture, and the residence times are long compared to the reaction times. The reactor contains four side ports. Two, which have Brewster angle MgF_2 windows, are used for entrance and exit of the photolysis beam from a Questek series 2000 excimer laser. The 193 nm laser radiation is focused through a plano-convex lens on the center of the reaction zone. The chemiluminescence is observed through ports aligned at right angles to the laser beam path. A Thorn EMI G26E314LF photomultiplier tube, PMT, is connected to a port to measure radiation in the 110−200 nm region through a MgF_2 window and a connector tube through which N_2 flows. The other port has a quartz window for observation in the 420−620 nm region with a Thorn EMI 9813QB PMT. A Corning 3389 filter is placed in front of the PMT to cut off shorter wavelength radiation. This lower limit was somewhat arbitrarily selected, on the basis of RMW, as our spectral measurements were obtained later. The upper limit is due to the PMT sensitivity. In a few experiments, mentioned below, this filter was replaced by others for narrower wavelength range measurements. The PMT signals were transferred via an amplifier-discriminator to a multichannel scaler and transferred for analysis and storage.

The methods followed for the rate coefficient measurements were the same as for earlier work where fluorescence or absorption monitoring of the transient reactants was used.[18−23] Thus, on the basis of the pseudo-first-order assumption $[C_2] \ll [O_2]$, chemiluminescence intensity I, proportional to $[C_2]$, can be written after background subtraction as

$$I = I_0 \exp(-k_{ps1}t) \qquad (2)$$

Here I_0 is the intensity at time $t = 0$ and k_{ps1} is the pseudo-first-order rate coefficient. The values of k_{ps1} are obtained by fitting[24] observed I vs t profiles to eq 2, Figure 4a. The exponentiality of such plots is checked by a two-stage residual analysis.[25] Only those experiments that pass this test are retained. Typically five or six k_{ps1} measurements at varying $[O_2]$ were used to obtain k_i, the rate coefficient of reaction 1, at the temperature and pressure of the experiment, Figure 4b.

To obtain the pressure dependence of the radiation intensities, the total intensity I_t, proportional to the area of the signal, was obtained by integrating eq 2 from $t = 0$ to $t = \infty$, which yields

$$I_t \propto I_0/k_{ps1} \qquad (3)$$

These I_t are then normalized and plotted against pressure. However, the pressure dependence obtained is not the true dependence of the chemiluminescence since the reaction zone

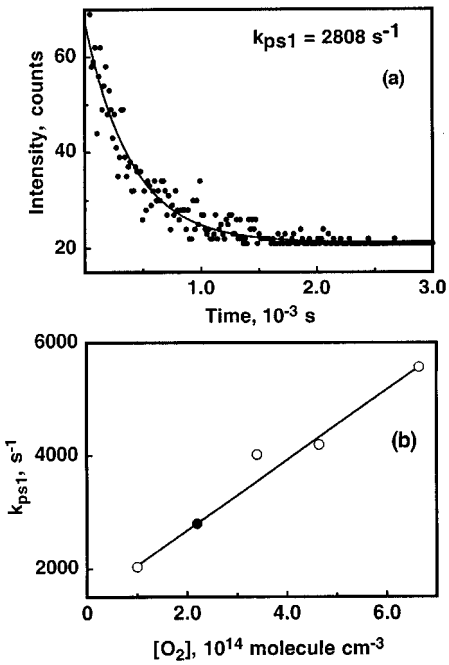

Figure 4. (a) Exponential decay plot of the CO 4+ intensity versus time after laser pulse. Conditions: $P = 26.9$ mbar; $T = 426$ K; $[C_2Cl_4] = 6.1 \times 10^{13}$; $[O_2] = 1.7 \times 10^{14}$ molecule cm^{-3}. (b) Rate coefficient determination. The darkened point corresponds to the result of (a).

is geometrically restricted. As a result, an increase in pressure will cause an increased amount of the reaction events to be observed. To eliminate this problem the $C_2 + O_2$ chemiluminescence was measured alternately at the same temperature and pressure as that from $O + NO \rightarrow NO_2 + h\nu$, a pressure-independent reaction in the range used.[26,27] The intensity ratio $I(CO)/I(NO_2)$ then closely approximates the correct pressure dependence of reaction 1. As the diffusion coefficients for the species involved in the two reactions are not the same, this procedure cannot be fully quantitative. To validate the method, experiments on the $O + C_2H_2$ reaction, discussed below, were made. These show that the correct dependence is closely approximated. The O atoms were produced by 193 nm single-photon photolysis of SO_2. Ar, O_2/Ar mixtures, and C_2Cl_4/Ar mixtures were obtained as above. The other gases were NO (99%), SO_2 (99.98%), and CO_2 (99.98%), all from Matheson.

Results

Flow Tube Spectral Measurements. The measurements were made with the C_2Cl_4/O_2 inlet facing the MgF_2 window, which gave maximum intensities. Band head assignments for both the VUV and the vis CO spectra were taken from refs 28 and 29. A VUV spectrum, obtained using the CCD camera, is shown in Figure 5a. The lowest and highest wavelengths observed are 131.6 nm (12,2) and 250 nm (10,20), respectively. The (13,5) transition has the largest observed v′ level, which corresponds to an excitation energy of 10.1 eV, well less than the reaction exoergicity. For comparison, a CO 4+ spectrum for the $O + C_2H_2$ reaction is shown in Figure 5b. The same band heads are present with comparable relative intensities. However, in the $C_2 + O_2$ case, the bands are broadened (i.e., tail off more gradually to longer wavelengths) and there is an apparent underlying continuum. The continuum could simply be attributed to a lack of resolution but could also be indicative of another emitter, such as a polyatomic reaction intermediate.

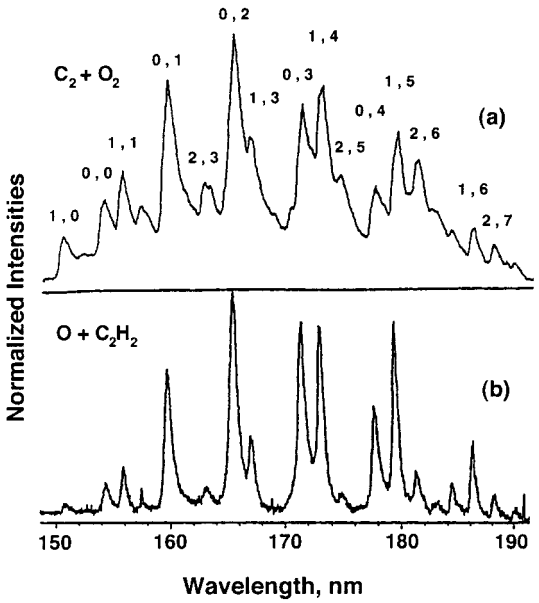

Figure 5. CO 4+ emission from $C_2 + O_2$ and $O + C_2H_2$. (a) $C_2 + O_2$: $P = 2.7$ mbar, $T = 493$ K, $\bar{v} = 8.8$ m s^{-1}; $[N_2] = 3.9 \times 10^{16}$, $[C_2Cl_4] = 5.4 \times 10^{12}$, $[O_2] = 5.8 \times 10^{14}$ molecule cm^{-3}; inlet-to-observation-window distance = 3 cm; slit width = 0.2 mm. (b) $O + C_2H_2$: $P = 12.0$ mbar, $T = 293$ K, $\bar{v} = 4.5$ m s^{-1}; $[Ar] = 2.9 \times 10^{17}$, $[C_2H_2] = 3.3 \times 10^{14}$, $[O_2] = 4.9 \times 10^{14}$ molecule cm^{-3}; inlet-to-observation-window distance = 3 cm; slit width = 0.2 mm.

The influence of changing reaction conditions on the spectral distribution of the VUV spectrum from $C_2 + O_2$ was investigated in a series of experiments, using the CCD camera, by normalizing peak heights relative to the CO 4+ (1,4) transition at 172.9 nm. Varying $[O_2]$ by a factor of 30 at 2.2 and 8.5 mbar, $[C_2Cl_4]$ by a factor of 10 at 2.1 and 9.3 mbar, and pressure from 2.7 to 10.7 mbar at constant $[C_2Cl_4]$ and $[O_2]$ yielded average variations in the spectral distribution of no more than (49 ± 33)%, where the uncertainty is given at the 2σ level. These changes did not noticeably affect the width of the individual bands and the continuum remained present under all conditions. The highest pressure here is comparable to that from $O + C_2H_2$, Figure 5b. The different appearance of the spectrum from that reaction is thus not due to a pressure effect. In a separate experiment, using the PMT as the detector, the spectrum of that reaction at ambient temperature was compared to that at 465 K at the same pressure and concentrations. No changes in the spectral distribution with temperature were observed either.

The influence of pressure on the absolute intensity was investigated at constant $[O_2]$ and $[C_2Cl_4]$. The pressure range covered was 2.7 to 13.3 mbar, with a simultaneous decrease in the average gas velocity $\bar{v}$ from 8.8 to 1.7 m s^{-1}. Visual observation indicated the extent of the glow to decrease from about 4 to 2 cm downstream from the inlet. Though the glow was thus more concentrated, the intensity of the 4+ bands decreased. For the (1,4) band the decrease was by 91%. Though this method of assessing the influence of pressure on emission intensity is not as accurate as are the HTP experiments of the next section, which were designed for that purpose, the agreement with the results given there is excellent.

A vis spectrum (390−900 nm) is shown in Figure 6a. Little radiation was detected at lower wavelengths; the upper limit is determined by the sensitivity of the CCD camera. In the figure, some of the strongest peaks are cut off as the sensitivity was chosen so as to show the maximum number of the weaker transitions. Strong emissions from the CO Triplet (d−a) and

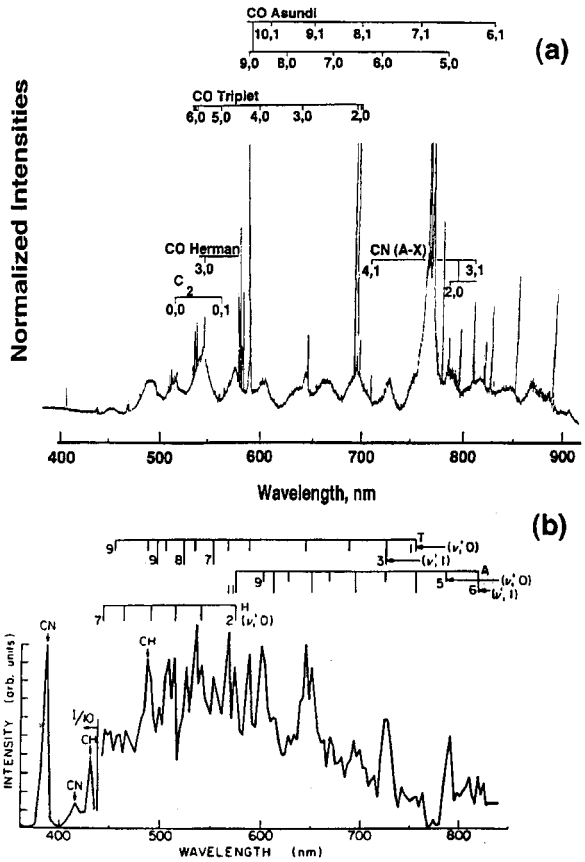

Figure 6. Visible emissions of $C_2 + O_2$ from the present study (upper panel) and from RMW. (a) Present work: $P = 2.3$ mbar, $T = 516$ K, $\bar{v} = 10.9$ m s^{-1}; $[N_2] = 4.1 \times 10^{16}$, $[C_2Cl_4] = 4.4 \times 10^{12}$, $[O_2] = 4.7 \times 10^{14}$ molecule cm^{-3}; slit width = 0.2 mm. Note that the peaks at 768 and 771 nm have been cut off. (b) RMW: $P = 1.7$ mbar, $T =$ ambient; $[Ar] = 2.3 \times 10^{16}$, $[C_2H_3CN] = 1.2 \times 10^{15}$, $[O_2] = 2.3 \times 10^{16}$ molecule cm^{-3}. A, T, and H, denote the Asundi, Triplet, and Herman bands, respectively. Reproduced from Figure 2 of ref 10 by permission from Elsevier Science and the authors of that article. Copyright 1980.

CO Asundi (a′−a) band systems are present as are medium strength emissions from the CO Herman (e−a) and C_2 Swan (A−X) systems. At high sensitivity the Asundi (22,2) band, corresponding to 9.57 eV excitation energy, was also evident. Only the certain band system attributions are shown. The unassigned peaks in the 800−900 nm region are possibly from the K_2 (A−X) system.[30] Very weak emission from K_2, CN, and OH was observed in the 290−390 nm wavelength range. A study of the $K + C_2Cl_4$ reaction, under other conditions, had shown the presence of broad peaks of $K^+C_2^-$ at 450, 495, and 535 nm.[31,32] There was no evidence for these in the present work.

RMW also measured the visible spectrum of the $C_2 + O_2$ reaction, as shown in Figure 6b. They produced C_2 by infrared multiphoton dissociation (IRMPD) of C_2H_3CN, under which conditions strong CH and CN emission also occur and a rather different spectral distribution is observed. Particularly, in their case the Herman bands are of similar intensity as the triplet and Asundi bands and there is a strong underlying continuum, not found in the present work. The latter could be due to the difference in full spectral bandwidth which was 2 nm for RMW and 0.33 nm in the present work.

HTP Emission Intensity Measurements. In Figure 7 the pressure dependence of the CO 4+ intensity from the $O + C_2H_2$ reaction is shown. It qualitatively agrees very well with the flow

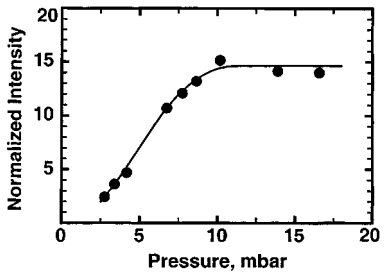

Figure 7. Wavelength-integrated CO 4+ intensity versus pressure for $O + C_2H_2$: T = ambient; $[SO_2] = 9.9 \times 10^{12}$ molecule cm^{-3}; $[C_2H_2] = 3.2 \times 10^{14}$ molecule cm^{-3}.

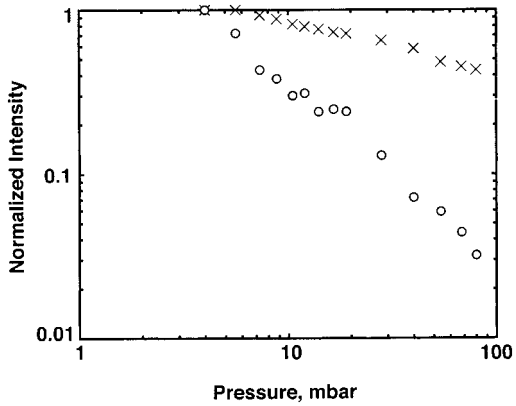

Figure 8. Comparison of the $C_2 + O_2$ normalized VUV (○) and vis (×) intensities as a function of pressure: T = ambient; $[C_2Cl_4] = 1.0 \times 10^{13}$; $[O_2] = 3.0 \times 10^{14}$ molecule cm^{-3}; bath gas Ar.

reactor measurements of Fontijn and Johnson,[4] where an initial rise with increasing Ar pressure, followed by a leveling out around 10 mbar, also was observed. This verifies the validity of the HTP method for measuring the intensity dependence on pressure. The fact that the measurements do not go through the origin shows that the method to compare to the O/NO reaction is, as suggested above, not fully quantitative.

The CO 4+ intensity from $C_2 + O_2$ decreases with pressure in the same regime, Figure 8, indicating that the predominant CO($A^1\Pi$) formation mechanism there is not collision-induced cross-relaxation from triplet states. The experiments have been repeated using (i) C_2H_2 as the photolytic precursor, (ii) CO_2 as bath gas, and (iii) temperatures up to 740 K. The results show similar intensity decreases with increasing pressure. Experiments with C_2H_2 using single photon photolysis have also been performed. This is known to lead to C_2H but not C_2.[33] No VUV luminescence was observed under these conditions.

Also shown in Figure 8 is the pressure dependence of the $C_2 + O_2$ vis chemiluminescence. This shows that the VUV is quenched more strongly. Different $[C_2Cl_4]/[O_2]$ ratios gave the same result. The radiative lifetime of CO($A^1\Pi$) is 1.1×10^{-8} s,[28] during which interval one molecule would, on average, undergo one collision at about 13 mbar. However, it can be seen that quenching takes place at much lower pressures. Moreover, the quenching efficiency of CO($A^1\Pi$, $v = 0$) by Ar is only 8×10^{-2} of gas kinetic.[34] This smaller quenching efficiency of Ar, compared to some other gases, can qualitatively also be seen from Figure 3 of Fontijn and Johnson.[4] Thus, the quenching shown by Figure 8 indicates that a precursor of CO($A^1\Pi$) is quenched.

Rate Coefficient Measurements. The rate coefficients for reaction 1 were measured by monitoring the chemiluminescence in the VUV and in the visible regions using C_2Cl_4 as the photolyte. In many experiments these were obtained simultaneously. The reaction conditions and results are shown in Table 1. The independence of the individual rate coefficients k_i from reaction parameters, other than temperature, was checked and confirmed by examining plots of $[k(T) - k_i]/k(T)$ versus these parameters. Thus the results are independent of pressure P and the corresponding total concentration [M], photolyte concentration $[C_2Cl_4]$, laser power, laser frequency, and stock gas mixtures used. The distance from the cooled inlet to the observation zone and the average gas velocities used were varied from 18 to 24 cm and from 14 to 25 cm s^{-1}, respectively. In addition, a few experiments over a more limited wavelength region than 420−620 nm were made by using Corning filters 5113 and 3480, which cut off radiation at wavelengths above 480 nm and below 560 nm, respectively. These yielded similar results in good agreement with RMW, who observed no difference between the room-temperature rate coefficients for the 500−800 nm range and those for wavelengths centered at 560, 725, and 790 nm.

Figure 9 shows the present data fitted by the Marquardt algorithm[35] to the form $A \exp(-E_a/RT)$ where $\pm\sigma_{ki}$ and $\pm\sigma_T/T = 2\%$ contribute to the weighing of each point. The fitted expression from the VUV data is

$$k_{VUV}(298-976\ \mathrm{K}) = 2.01 \times 10^{-11} \exp(-503\ \mathrm{K}/T)\ \mathrm{cm}^3\ \mathrm{molecule}^{-1}\ \mathrm{s}^{-1} \quad (4)$$

The variances and covariance are $\sigma_A^2 = 1.21 \times 10^{-3}$ A^2, $\sigma_E^2 = 3.64 \times 10^2$, and $\sigma_{AE} = 0.63$ A. These variances and covariance are combined by the method of Wentworth,[36] to yield a 2σ precision level of ±2% to ±7%, depending on temperature. Allowing ±20% for any unrecognized systematic errors then leads to a 2σ accuracy level of ±21%. The vis data similarly yield

$$k_{vis}(298-711\ \mathrm{K}) = 1.10 \times 10^{-11} \exp(-381\ \mathrm{K}/T)\ \mathrm{cm}^3\ \mathrm{molecule}^{-1}\ \mathrm{s}^{-1} \quad (5)$$

with $\sigma_A^2 = 1.87 \times 10^{-3}$ A^2, $\sigma_E^2 = 3.93 \times 10^2$, and $\sigma_{AE} = 0.83$ A, with 2σ precision limits of ±2% to ±5% and a corresponding confidence limit of ±21%.

The k_{vis} data may be seen, Figure 9, to be in excellent agreement with LIF measurements of C_2 ($a^3\ \Pi$) consumption by Baughcum and Oldenborg,[12] LIF experiments on C_2 ($X^1\Sigma$) and Asundi chemiluminescence emission by Pitts et al.,[15] $^3C_2$ and $^1C_2$ LIF measurements and CO triplet emission experiments by RMW, the LIF measurements on $^3C_2$ of Donnelly and Pasternack[14] and Filseth et al.,[9] and those of $^3C_2$ and $^1C_2$ by Pasternack and McDonald.[13] Fitting all these data yields

$$k_{vis/LIF}(293-1250\ \mathrm{K}) = 1.13 \times 10^{-11} \exp(-392\ \mathrm{K}/T)\ \mathrm{cm}^3\ \mathrm{molecule}^{-1}\ \mathrm{s}^{-1} \quad (6)$$

which is nearly identical to eq 5. However, the VUV measurements consistently give somewhat higher values. This could be an experimental artifact, as discussed below.

Discussion

The quenching behavior of the 4+ emission indicates that an intermediate species is involved in the process leading to CO ($A^1\Pi$). This is in accord with the orbital symmetry argument of RMW that the "CO products are formed via a mechanism in which one bond is formed initially and subsequently the C_2O_2 transition complex rotates and rearranges itself so that a second bond is formed and the products separate." It is thus probable

TABLE 1: Summary of Rate Coefficients Measurements of $C_2 + O_2$

T[a] (K)	P (mbar)	[M] (10^{18} cm^{-3})	[C_2Cl_4] (10^{14} cm^{-3})	[O_2] (10^{14} cm^{-3})	k_{VUV} (cm^3 molecule^{-1} s^{-1})	k_{vis} (cm^3 molecule^{-1} s^{-1})
298[b,e,j]	26.7	0.65	0.61	1.70−6.00[o]		2.84×10^{-12}
298[f,j]	26.7	0.65	0.61	1.70−6.00[o]	4.43×10^{-12}	
299[c,g,k]	160	3.87	0.61	1.70−6.00[o]		3.11×10^{-12}
299[c,i,l]	160	3.87	0.61	1.70−6.00[o]		3.06×10^{-12}
299[c,h,j]	26.7	0.65	0.61	1.70−6.00[o]		2.94×10^{-12}
300[c,f,j]	26.7	0.64	0.61	1.70−6.00[o]	5.05×10^{-12}	3.24×10^{-12}
300[i, j]	339	8.17	2.13	9.27−67.4[p]	3.73×10^{-12}	
303[c,i,j]	26.7	0.64	0.61	1.70−6.00[o]		3.66×10^{-12}
310[i, j]	112	2.61	1.25	2.04−7.78[o]	4.86×10^{-12}	
327[b,i,j]	26.7	0.59	1.00[n]	1.00−12.00[q]		3.29×10^{-12}
331[c,i,j]	13.3	0.29	1.00[n]	6.00−15.00[p]	4.47×10^{-12}	3.01×10^{-12}
348[i,j]	204	4.24	2.13	2.98−10.0[o]	5.56×10^{-12}	
364[c, i, j]	293	5.83	2.20	3.00−15.0[o]	5.85×10^{-12}	3.37×10^{-12}
385[c,g,j]	200	3.76	0.72	2.20−6.00[o]		4.63×10^{-12}
386[i, j]	139	2.60	2.40	4.08−15.6[q]	6.17×10^{-12}	
401[i, j]	279	5.03	1.87	4.58−17.3[o]	5.18×10^{-12}	
403[b, i, j]	26.7	0.48	0.55	1.00−6.70[o]		4.73×10^{-12}
414[c, i, j]	187	3.26	1.50	4.00−16.0[o]	6.59×10^{-12}	3.44×10^{-12}
414[i, j]	373	6.53	1.50	3.00−15.0[o]	4.86×10^{-12}	
426[i, j]	26.7	0.45	0.61	1.70−6.00[o]	6.05×10^{-12}	
426[i, j]	141	2.40	0.35	1.82−13.3[p]	6.30×10^{-12}	
427[c,j,m]	160	2.71	0.61	1.70−6.00[o]		4.85×10^{-12}
429[d,i,j]	200	3.37	0.63	1.90−6.00[o]	8.02×10^{-12}	4.58×10^{-12}
429[d,i,j]	13.3	0.23	0.41	1.29−7.98[q]	6.57×10^{-12}	4.56×10^{-12}
435[d, i, j]	200	3.33	0.63	1.90−6.00[o]	7.72×10^{-12}	4.37×10^{-12}
472[d,e,j]	200	3.07	0.63	1.90−6.00[o]	6.68×10^{-12}	5.60×10^{-12}
475[i, j]	200	3.05	0.63	1.90−6.00[o]	6.33×10^{-12}	
494[i,j]	133	1.95	1.80	3.00−12.0[o]	6.90×10^{-12}	
497[i,j]	276	4.02	1.92	3.33−12.9[q]	6.75×10^{-12}	
499[b,i,j]	26.7	0.39	0.61	1.70−6.00[o]		5.80×10^{-12}
519[c,i,j]	13.3	0.19	0.31	0.90−5.90[q]	7.12×10^{-12}	4.81×10^{-12}
520[b, i, j]	26.7	0.37	0.45	0.90−5.80[o]		5.50×10^{-12}
535[b, i, j]	200	2.71	0.72	1.50−6.00[o]		6.20×10^{-12}
548[c, i, j]	26.7	0.35	0.61	1.70−6.00[o]		5.18×10^{-12}
556[c, i, j]	200	2.60	0.72	1.50−6.00[o]		4.81×10^{-12}
558[b, i, j]	200	2.59	0.60	1.10−6.00[o]		4.5×10^{-12}
567[i, j]	187	2.38	0.60	1.10−6.00[o]	8.21×10^{-12}	
570[c, i, j]	187	2.37	0.61	1.70−6.00[o]	10.3×10^{-12}	6.29×10^{-12}
579[d, i, j]	200	2.50	0.60	1.10−6.00[o]		5.19×10^{-12}
584[i, j]	256	3.17	1.77	2.03−7.79[o]	8.23×10^{-12}	
608[c, i, j]	13.3	0.16	0.31	0.94−5.70[q]	10.5×10^{-12}	6.56×10^{-12}
609[d, i, j]	187	2.22	1.50	2.00−7.00[o]	7.57×10^{-12}	5.74×10^{-12}
618[c, i, j]	201	2.36	0.60	1.10−6.00[o]		5.09×10^{-12}
633[i, j]	200	2.29	0.72	1.50−6.00[o]	9.61×10^{-12}	
680[i, j]	187	1.99	0.60	1.10−6.00[o]	10.1×10^{-12}	
711[c,i,j]	13.3	0.14	0.50[n]	0.80−4.80[q]	11.4×10^{-12}	7.69×10^{-12}
836[i, j]	143	1.24	0.50	1.12−4.25[o]	11.31×10^{-12}	
976[i, j]	109	0.81	0.57	0.57−2.18[o]	12.23×10^{-12}	

[a] $\sigma_T/T = \pm 2\%$. [b] Measurements in the visible conducted using a Corning 5113 glass filter. [c] Measurements in the visible conducted using a Corning 3389 glass filter. [d] Measurements in the visible conducted using a Corning 3480 glass filter. [e] Measurements conducted using a repetition rate of 4.0 Hz. [f] Measurements conducted using a repetition rate of 2.0 Hz. [g] Measurements conducted using a repetition rate of 5.0 Hz. [h] Measurements conducted using a repetition rate of 6.0 Hz. [i] Measurements conducted using a repetition rate of 3.0 Hz. [j] Measurements conducted using the full laser power. [k] Measurements conducted using 22.2% of the full laser power. [l] Measurements conducted using 33.3% of the full laser power. [m] Measurements conducted using 55.5% of the full laser power. [n] A 2% C_2Cl_4/Ar mixture was used; in all other measurements a 1% C_2Cl_4/Ar mixture was used. [o] A 0.5% O_2/Ar mixture was used. [p] A 5% O_2/Ar mixture was used. [q] A 1% O_2/Ar mixture was used.

that the triplet emitters formation also involves a C_2O_2 complex; there is no direct evidence for this from the quenching experiments as, because of the relatively long lifetimes involved ($\tau_{rad}(CO(a'\,^3\Sigma^+)) = 5 \times 10^{-6}$ s, $\tau_{rad}(CO(d\,^3\Delta) \sim 7 \times 10^{-6}$ s),[37] direct quenching of the emitters could be significant.

The exoergicity of reaction 1 is such that if one CO molecule is formed in an electronically excited state, the other must form in the singlet ground state. Spin-conservation then demands that the $^3C_2$ is responsible for the 4+ emission, while both $^1C_2$ and $^3C_2$ states could lead to triplet complexes, and thus to triplet emitters. MRW have offered evidence under other conditions (see below) that the triplet emitters mostly (80−90%) originate from $^1C_2$. The pathways are further interconnected by the $^1C_2$, $^3C_2$ equilibration in the presence of O_2. The following scheme combines these observations:

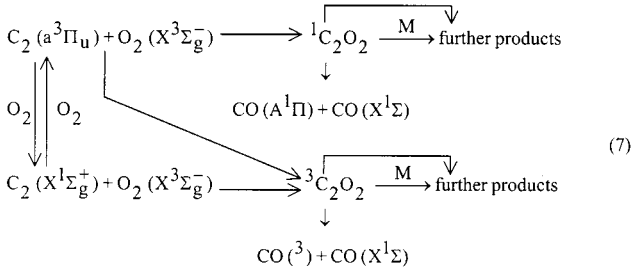

(7)

Various $^1C_2O_2$ and $^3C_2O_2$ structures could be involved. The

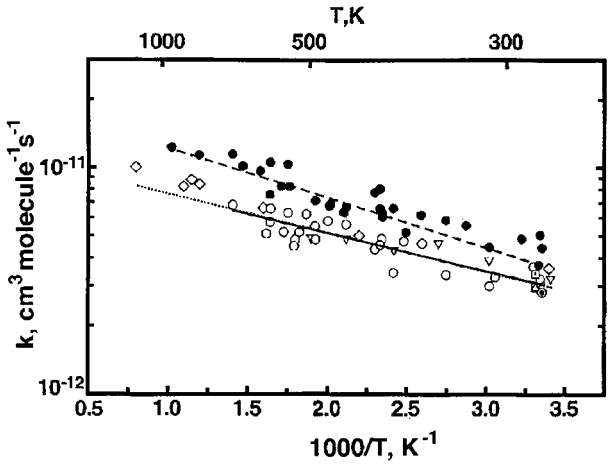

Figure 9. Summary of $C_2 + O_2$ rate coefficient measurements: ●, CO 4+ emission and (---) fit, eq 4, present data, 193 nm MPD; ○ visible emission and (—) fit, eq 5, present data, 193 nm MPD; ▪▪▪, best fit eq 6 to all data but CO 4+; ◊, Baughcum and Oldenborg, $^3C_2(v = 0)$ LIF, 193 nm MPD; ▽, Pitts et al., $^1C_2(v = 0)$ LIF and Asundi emission, 193 nm MPD; □, Reisler et al., $^3C_2(v = 0)$ and $^1C_2(v = 0)$ LIF and CO triplet emission, IRMPD; △, Donnelly and Pasternack, $^3C_2(v = 0)$ LIF, 193 nm MPD; ⊡, Filseth et al., $^3C_2(v = 0)$ LIF, IRMPD; ⊙, Pasternack and McDonald, $^1C_2(v = 0)$ LIF, 193 nm MPD.

observation on the $O + C_2H_2$ reaction that collision-induced cross relaxation of the CO triplet states can populate the $A^1\Pi$ state indicates that this will occur also to some degree in the present system. However, the different pressure dependences in the same low-pressure range for the two reactions, Figures 7 and 8, indicates that this is not a major contributor to the $C_2 + O_2$ VUV emission.

Scheme (7) could suggest that the higher k_{VUV} values compared to the rate coefficients from the other methods is due to a faster $^3C_2$ reaction and that the equilibrium between $^1C_2$ and $^3C_2$ cannot keep pace. This, however, is uncertain. MRW have reported that at $[O_2] = 3.3 \times 10^{14}$ molecule cm^{-3} complete equilibrium is not achieved at least at early ($<10^{-4}$ s) reaction times and that $^1C_2$ reacts faster. Their experiments were done by IRMPD of C_2H_3CN in the presence of a high CH_4 concentration (3.3×10^{15} molecule cm^{-3}). CH_4 was used as a scavenger which removes $^1C_2$ much faster than $^3C_2$. The IRMPD experiments result in relatively low $^3C_2$ vibrational and rotational temperatures of 700 and 600 K, respectively.[38] It is thus conceivable that in the present photolysis experiments $^3C_2$ is formed with more internal energy, resulting in slightly higher rate coefficients. Baughcum and Oldenborg[12] have measured the $^3C_2 + O_2$ rate coefficients in 26 mbar He from 298 to 1300 K using 193 nm MPD of CF_3CCCF_3. They found that at 298 K $^3C_2(v = 1, 2)$ reacted about twice as fast as the $v = 0$ molecules but that by about 750 K the difference in the rate coefficients is small. The observations of Figure 9 show closely the same difference between k_{VUV} and the other measurements over the entire temperature range. Hence, k_{VUV} does not appear to have been influenced by vibrational excitation of $^3C_2$, but electronically excited $^3C_2$ could have formed in the UV photolysis. Filseth et al., in a room-temperature experiment over the $[O_2] = 7 \times 10^{14}-7 \times 10^{15}$ molecule cm^{-3} range, found that the VUV and the $^3C_2$ LIF observation yield the same rates.[9] Their observations were made using IRMPD of C_2H_3CN, similarly to MRW, but without added hydrocarbon.

MRW also reported an increase in the VUV emission relative to the visible intensities upon increase in Ar pressure and tentatively attributed this to CO intersystem crossing. These experiments were done with a filter PMT combination covering the ≈170−350 nm region. Thus, only the longer wavelength tail of the CO 4+ spectrum was observed and interfering emissions in the 200−350 nm region could have been present. They allowed that the high $[O_2] = 3.3 \times 10^{15}$ molecule cm^{-3} might have been responsible for this observation and consider this experiment to be inconclusive.[39] If it is correctly interpreted, then this intersystem crossing effect is the same as observed for $O + C_2H_2$[4,6] but is contrary to the present HTP and flow tube $C_2 + O_2$ observations. Once either the $CO(A^1\Pi)$ or the triplet states are present, intersystem crossing will occur. Its influence on the fourth positive over triplet emission intensity ratios should depend on conditions. In the $O + C_2H_2$ case, and under the specific conditions of MRW, the processes leading to triplet states appear favored; under the conditions of the present experiments, such is not the case. This difference between the IRMPD and the present work may also explain the different spectral distribution and the continuum observed by RMW. If the continuum would be due to a polyatomic emitter, for which excited $^3C_2O_2$ is a likely candidate, less of it would have formed in the present work. One may then further speculate that the VUV continuum from $C_2 + O_2$ is due to a $^1C_2O_2$ transition. The ground state of $^1C_2O_2$ is repulsive and the triplet ground-state molecules dissociate within a few nanoseconds by curve-crossing to the singlet surface.[40] The continuum of Figure 5a may thus be excimer radiation.

In addition to two rovibrationally excited CO ($X^1\Sigma$) molecules, the possible direct "further products" of eq 7 are C_2O_2, $C_2O + O$, and $CO_2 + C$, which could be in excited states. These sets of products represent exothermic and spin-allowed paths. Of particular interest here is

$$^{1,3}C_2 + O_2(X^3\Sigma) \rightarrow {}^{1,3}C_2O_2 \rightarrow {}^{1,3}C_2O + O(^3P) \qquad (8)$$

which is 2.1 eV exothermic for $C_2O(X^3\Sigma)$ formation and 0.65 and 1.0 eV less exothermic for C_2O $\tilde{a}^1\Delta$ and $b^1\Sigma$ formation, respectively. These products are the same reactants responsible for the CO 4+ and triplet emissions in the $O + C_2H_2$ and C_3O_2 reactions,[2−6] the mechanism for which has recently been indicated to be[6]

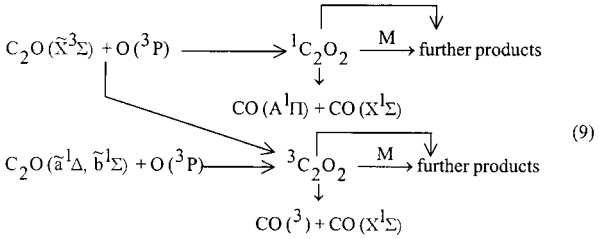

(9)

The band intensity distributions of the 4+ bands from schemes (7) and (9) are very similar, Figure 5. This would suggest similar configurations for the C_2O_2 complexes at the point of dissociation to two CO. For (7) the formation of the first new bond would result in a CCOO complex, but the subsequent rotation and rearrangement[10] has to lead to an OCCO structure before the dissociation. Such a structure also should form from scheme (9). Ab initio calculations would be helpful to determine and compare these C_2O_2 intermediates.

Some contribution from $C_2O + O$ from (9) to the observed emissions from $C_2 + O_2$ cannot be excluded. However, this cannot be significant. This would require that C_2O_2 would have to be produced twice before emission occurs, which should have resulted in a rise before the decrease in 4+ intensity vs time plots, contrary to what is found; see Figure 4a. Such a rise is evident in I(CO 4+) vs t plots of $O + C_2H_2$ in the same

apparatus, indicative of the buildup of ^3C_2O. The opposite pressure dependence of the CO 4+ bands from the two processes also argues against this. The pressure dependence of the visible emission intensities from both reactions also differ. Those from $C_2 + O_2$ can be seen to approximate a $\log I \propto -\log P$ relationship, Figure 8. For the triplet bands of $O + C_2H_2$, an $I \propto -P$ relationship was found albeit over a narrow range, 2−10 mbar.[6] Finally, the 4+ spectra from $C_2 + O_2$, though having a similar vibrational distribution as those from $O + C_2H_2$, have considerably broadened bands and the underlying apparent continuum.

The previous $C_2 + O_2$ rate coefficient measurements[9,10,12−15] together have covered the 1−65 mbar range. The pressure independence of the reaction rate coefficients has been confirmed in the present work up to severalfold higher pressures. The reaction has also been studied by Kruse and Roth in a shock tube over the 2750−3950 K range, at pressures of 1.7−2.3 bar.[16] Under these conditions a radically different $k(T)$ expression is obtained, $2.8 \times 10^{-10} \exp(-4070\ \mathrm{K}/T)$ cm^3 molecule^{-1} s^{-1}. On the basis of the common assumption, from the literature data of Figure 9, that the products are 2 CO, they suggested that the $C_2O + O$ and/or $CO_2 + C$ channels may dominate under their conditions, which appears reasonable. Their C_2 investigations have also led to the suggestion that the JANAF $\Delta H^o_{298.15}$ value for C_2 has to be reduced by about 0.24 eV.[41] This would reduce the reaction exothermicities given in this paper by this amount but would not affect any of the arguments.

Concluding Remarks

This work has demonstrated that the VUV emission from $C_2 + O_2$ is dominated by the CO 4+ bands. A method has been developed to study the pressure dependence of chemiluminescence intensities in a pseudostatic cell, notwithstanding that pressure influences the geometrical distribution of the observed glow. The pressure dependence of the CO 4+ intensities from $C_2 + O_2$ is, under similar circumstances, the opposite of that from the $O + C_2O$ reaction. This indicates that direct ($A^1\Pi$) formation, as compared to its production by intersystem crossing, is more important in the $C_2 + O_2$ than in the $C_2O + O$ reaction under the present conditions. The basic reaction paths suggested here, initial C_2O_2 formation followed by dissociation to produce electronically excited and ground electronic state CO molecules, are very similar for both reactions. Ab initio studies to determine energies and geometries of the various possible C_2O_2 structures, their isomerization, and barriers for dissociation are recommended. Other open questions for the $C_2 + O_2$ system are what fraction of the reaction events leads to excited CO formation and what is the importance of the 2 CO versus the $O + C_2O$ and $CO_2 + C$ reaction channels in the "low" (300−1300 K) and "high" (≈3000 K) temperature overall kinetics.

Acknowledgment. This work is supported by AFOSR under Grants F29620-98-1-0047 and -0410, Dr. M. A. Birkan, Program Manager. We thank Dr. K. D. Bayes for helpful discussions and Dr. G. Dorthe for showing us the $K + C_2Cl_4$ method for flow reactor C_2 production before publication. We also thank Dr. A. Goumri for participation with some preliminary experiments and W. F. Flaherty for assistance throughout this work. Three Rensselaer undergraduates, M. L. Nardone, I. Dissanayake, and L. Huang assisted with the spectral work.

References and Notes

(1) Gaydon, A. G. *The Spectroscopy of Flames*, 2nd ed.; Chapman and Hall: London, 1974; p 155 ff.
(2) Becker, K. H.; Bayes, K. D. *J. Chem. Phys*. **1968**, *48*, 653.
(3) Bayes, K. D. *J. Chem. Phys*. **1970**, *52*, 1093.
(4) Fontijn, A.; Johnson, S. E. *J. Chem. Phys*. **1973**, *59*, 6193.
(5) Burke, M. L.; Dimpfl, W. L.; Sheaffer, P. M.; Zittel, P. F.; Bernstein, L. S. *J. Phys. Chem.* **1996**, *100*, 138.
(6) Fontijn, A.; Goumri, A.; Brock, P. E., II. *Combust. Flame* **2000**, *121*, 699.
(7) Tilford, S. G.; Simmons, J. D. *J. Phys. Chem. Ref. Data* **1972**, *1*, 147.
(8) . Chase, M. W., Jr. *NIST-JANAF Thermochemical Tables*, 4th ed.; J. Phys. Chem. Ref. Data, Monograph 9; 1998.
(9) Filseth, S. V.; Hancock, G.; Fournier, J.; Meier, K. *Chem. Phys. Lett*. **1979**, *61*, 288.
(10) Reisler, H.; Mangir, M.; Wittig, C. *Chem. Phys*. **1980**, *47*, 49.
(11) Mangir, M. S.; Reisler, H.; Wittig, C. *J. Chem. Phys*. **1980**, *73*, 829.
(12) Baughcum, S. L.; Oldenborg, R. C. In *The Chemistry of Combustion Processes*; ACS Symposium Series 249; American Chemical Society: Washington, DC, 1984; p 257.
(13) Pasternack, L.; McDonald, J. R. *Chem. Phys*. **1979**, *43*, 173.
(14) Donnelly, V. M.; Pasternack, L. *Chem. Phys*. **1979**, *39*, 427.
(15) Pitts, W. M., Jr.; Pasternack, L.; McDonald, J. R. *Chem. Phys*. **1982**, *68*, 417.
(16) Kruse, T.; Roth, P. *27th Symposium (International) on Combustion*; The Combustion Institute: Pittsburgh, PA, 1998; p 193.
(17) Daugey, N.; Bergeat, A.; Schuck, A.; Caubet, P.; Dorthe, G. *Chem. Phys. Lett*. **1997**, *222*, 87.
(18) Mahmud, K.; Kim, J.-S.; Fontijn, A. *J. Phys. Chem*. **1990**, *94*, 2994.
(19) Fontijn, A., Futerko, P. M. In *Gas-Phase Metal Reactions*; Fontijn A., Ed.; North-Holland: Amsterdam, 1992; Chapter 6.
(20) Fontijn, A.; Blue, A. S.; Narayan, A. S.; Bajaj, P. N. *Combust. Sci. Technol*. **1994**, *101*, 59.
(21) Ko, T.; Marshall, P.; Fontijn, A. *J. Phys. Chem*. **1990**, *94*, 1401.
(22) Marshall, P.; Ko, T.; Fontijn, A. *J. Phys. Chem*. **1989**, *93*, 1922.
(23) Marshall, P., Narayan, A. S., Fontijn, A. *J. Phys. Chem.* **1990**, *94*, 2998.
(24) Marshall, P. *Comput. Chem*. **1987**, *11*, 219.
(25) Ko, T.; Adusei, G. Y.; Fontijn, A. *J. Phys. Chem*. **1991**, *95*, 8745. Fontijn, A.; Goumri, A.; Fernandez, A.; Anderson, W. R.; Meagher, N. *J. Phys. Chem.* **2000**, *104*, 6003.
(26) Fontijn, A.; Meyer, C. B.; Schiff, H. I. *J. Chem. Phys*. **1964**, *40*, 64.
(27) Becker, K. H., Groth, W.; Thran, D. *Chem. Phys. Lett*. **1972**, *15*, 215.
(28) Krupenie, P. H. *The Band Spectrum of Carbon Monoxide*; National Standard Reference Data Series, NSRDS-NBS 5; U.S. Government Printing Office: Washington, DC, 1966; p 74.
(29) Suchard, S. N., Ed. *Spectroscopic Data, Vol. 1 Heteronuclear Diatomic Molecules*; IFI/Plenum: New York, 1975; Part A.
(30) Pearse, R. W. B.; Gaydon, A. G. *The Identification of Molecular Spectra*, 4th ed.; Chapman and Hall: London, 1976.
(31) Balling, L. C.; Wright, J. J. *Chem. Phys. Lett*. **1982**, *87*, 139.
(32) Lin, K. K.; Balling, L. C., Wright, J. J. *Chem. Phys. Lett.* **1987**, *133*, 246.
(33) Renlund, R. M.; Shokoohi, F.; Reisler, H.; Wittig, C., *J. Phys. Chem.* **1982**, *86*, 4165.
(34) Fink, E. H.; Comes, F. J., *Chem. Phys. Lett.* **1972**, *14*, 433.
(35) Press: W. H.; Flannery, B. P.; Teukolsky, S. A.; Vetterling, W. T., *Numerical Recipes*; Cambridge University: Cambridge, U.K., 1986; Chapter 14.
(36) Wentworth, W. E. *J. Chem. Educ*. **1965**, *162*, 42, 96.
(37) Van Sprang, H. A.; Mohlman, G. R.; de Heer, F. J. *Chem. Phys.* **1977**, *24*, 429.
(38) Reisler, H.; Mangir, M.; Wittig, C. *J. Chem. Phys.* **1979**, *71*, 2109.
(39) Reisler, H. Private communication to A.F., July 2000.
(40) Schröder, D.; Heinemann, C.; Schwarz, H.; Harvey, J. N.; Dua, S.; Blanksby, S. J.; Bowie, J. H. *Chem. Eur. J.* **1998**, *4*, 2550
(41) Kruse, T.; Roth, P. *J. Phys. Chem.* **1997**, *101*, 2138.